

Preparation and Properties of Melt-Blended Polylactic Acid/ Polyethylene Glycol-Modified Silica Nanocomposites

Sun-Mou Lai, Jhong-Ren Chen, Jin-Lin Han, Yi-Fei Yu, Hui-Yu Lai

Department of Chemical and Materials Engineering, National I-Lan University, Taiwan, Republic of China

Correspondence to: S.-M. Lai (E-mail: smlai@niu.edu.tw)

ABSTRACT: One commercial type of fumed silica modified with methoxy polyethylene glycol (mPEG) plasticizer was incorporated into polylactic acid (PLA) biobased polymer to improve its performance. The modification on silica was confirmed through Fourier transform infrared spectra, nuclear magnetic resonance, and TGA assessments. The grafting percentage of mPEG onto silica was about 19.8 wt %. Transmission electron microscope revealed a similar degree of dispersion for control silica and modified silica-filled PLA nanocomposites. Not much difference in the glass transition temperatures at various silica contents was found for PLA/control silica systems from the differential scanning calorimetry measurement, but the glass transition temperature of PLA/modified silica nanocomposite at 10 phr of modified silica showed up to 11°C decrement. It was suggested that the mPEG plasticizer efficiently plasticized the PLA matrix through the enhanced segmental mobility of PLA chains. Young's modulus of PLA was about 2133 ± 53 MPa, and the value for the nanocomposite increased to 2547 ± 54 MPa at 10 of phr control silica mainly due to the reinforcing effect from nanoparticles. For modified silica, Young's modulus decreased at various silica contents. The elongation at break for modified silica-filled cases was higher than that of control silica-filled cases. These results were attributed to the plasticizing effect of surface modifier. Optical transmittance for pristine PLA was generally in a similar order as PLA/control silica and modified silica cases at various silica contents. The results agreed with the morphology observation as well. © 2013 Wiley Periodicals, Inc. *J. Appl. Polym. Sci.* 130: 496–503, 2013

KEYWORDS: biodegradable; mechanical properties; composites

Received 7 July 2012; accepted 15 February 2013; published online 19 March 2013

DOI: 10.1002/app.39183

INTRODUCTION

Nanocomposites formed through the hybrid of organic matrix and inorganic dispersed phase rendered significant advances in the development of polymer technology. Thus, much attention has been paid on the recent progress in light of the nanotechnology at the nanometer scale. In particular, it is imperative to enhance the interfacial interaction between polymer matrix and dispersed inorganic particles to make the most of the high surface area of nanoparticles in achieving the best properties. Philipp and Schmidt¹ and Wilkes et al.² conducted the pioneered research on the preparation of organically modified silicates (ORMOSIL or CERAMER) using various types of alkoxy silane via a sol-gel process to avoid the aggregation of nanoparticles due to the strong silanol (Si—OH) interactions between silicates and enhance the interfacial interaction between polymer matrix and dispersed particles. Tremendous works have applied a similar concept to alleviate the problem of particle aggregation in the academia and industries.

The growing environmental concern toward sustainable development has led to the uprising interests on the development of

biodegradable or biomass polymers.³ Polylactic acid (PLA) synthesized through the ring opening polymerization of lactide obtained from the fermentation of the sugar feedstock, such as corn, etc., has been valued as an important biomass polymer used in the biomedical and environmental applications in light of its biodegradability, biocompatibility, and nontoxicity.⁴ However, because of its brittleness and low thermal stability, etc., the novel development of PLA nanocomposites to further improve and enhance its related properties has been widely conducted recently.^{4–20}

Despite of numerous researches engaged in the development of nanoclay-filled systems,^{4–12} only limited PLA/silica nanocomposites were investigated recently in the literature.^{13–20} Yan et al.¹³ carried out the first study on the preparation of nanosilica grafted with lactic acid, which was then melt-blended with PLA to enhance the interfacial interaction and increase the elongation at break of the nanocomposites up to eight times. Yan et al.¹⁶ pointed out that the small amount of silica prepared by a sol-gel method could improve tensile strength of plasticized

PLA/silica nanocomposites in a great extent. Huang et al.^{17,18} suggested that nanoscale silica particles prepared via a sol-gel method appeared to act as a heterogeneous nucleation role to increase the crystallization of PLA, but microscale silica tended to inhibit the crystallization. Zhu et al.¹⁹ prepared PLA/SiO₂ nanocomposites using oleic acid-modified silica and reported that only 1% of modified silica could enhance the flexibility of PLA up to 3.2 times. The complex viscosity was analyzed to probe the particle aggregation of PLA/modified silica nanocomposites. However, no comparison on the neat silica-filled PLA system was reported.

To the authors' best knowledge, there is no literature available that discussed the effects of PEG-modified nanosilica on PLA/silica nanocomposites to illustrate the significance of surface effect under a melt-blended process. Instead of adding a common plasticizer into the PLA matrix, we tried to graft the plasticizer onto the silica surface to form plasticized silica by combining both plasticizing (plasticizer) and reinforcing (silica) effects to balance the performance of nanocomposites. In addition, the prevailing surface modification processes in the literature often led to high dispersion of silica, which made it hard to separate independently, the surface modification effect and silica dispersion effect. In this study, the selected commercial silica exhibited a high dispersion degree in the matrix. Even though the specific surface modification was carried out, the silica with or without surface modification still remained a similar dispersion in general. Therefore, a direct effect of the surface modifier on other properties could be elucidated under the similar silica dispersion after modification. This work aims to unveil this important observation further and focuses on thermal properties and tensile properties to contrast the significance of the surface modification role in this silica-filled nanocomposite system.

EXPERIMENTAL

Materials

The materials used in this study were poly(lactic acid) (PLA) and one commercial fumed silica (Aerosil), γ -glycidoxypropyltrimethoxy silane (GPS), and methoxy polyethylene glycol (mPEG). PLA with a D-isomer content of 12% and a density of 1.24 g/cm³ was supplied from NatureWorks LLC under the trade name of 4060D. Fumed Silica, Aerosil[®] A200, manufactured by Degussa, had a primary particle size of 12 nm. Aerosil[®] A200 with a density of 2.2 g/cm³ was hydrophilic fumed silica without any organic treatment. The silane coupling agent (GPS) and mPEG (molecular weight of 750 g/mole) obtained from Acros organics were used to modify the silica surface. All other reagents and solvents, including isopropyl alcohol (IPA), dichloromethane, and deionized water, were used as received.

Sample Preparations. The surface treatment of silica was modified based on the literature work.²¹ Five grams of silica were added into 250 mL of IPA solution, followed by a ultrasonic treatment for 30 min. Twenty-five grams of GPS were hydrolyzed in a solution at a weight ratio of water/GPS/IPA = 1.5/1/3 for 3 h. The hydrolysis solution was added to the silica/IPA mixture for grafting reaction under 70°C for 3 h. Then, the silica mixture was well mixed in a homogenizer for 30 min, followed by another ultrasonic treatment for 15 min. Afterwards,

the above mixture subjected to vacuum filtering was thoroughly washed with IPA for five times. The prepared GPS-silica was stored into the refrigerator for further use. For the mPEG grafting reaction, 5 g of prepared GPS-silica and 1.5 g of mPEG were added into in 250 mL of dichloromethane solution, which was well mixed by a homogenizer for 30 min. The homogeneous mixture was mixed with boron trifluoride etherate (BF₃·O(C₂H₅)₂) catalyst for the grafting reaction at -10°C for 45 min. Afterwards, the mPEG750-silica was obtained by vacuum filtering after a thorough IPA wash for two times. The bare silica was treated under the same procedure, denoted as control silica hereafter, to ensure the same thermal history for better comparison. For the preparation of composites, PLA and the modified silica [1, 4, 10 phr (parts per 100 resins)] were mixed using an internal mixer (Brabender 815605, Plastograph) under 10 rpm for first 3 min and 80 rpm for another 7 min at 160°C. For comparison, pristine PLA was also melt-blended as the reference material. The prepared batch was then hot-pressed at 160°C to obtain about 1 mm thick specimen. After their preparation, the samples were placed for at last one day in a vacuum drier before any measurements.

Measurements

Structure Characterizations. The Fourier transform infrared spectra (FTIR) of modified silica were recorded on spectrophotometer (Perkin Elmer, Spectrum 100) at a resolution of 4 cm⁻¹ for 32 scans from 400 to 4000 cm⁻¹. ¹³C MAS solid-state Nuclear magnetic resonance (NMR) experiments were performed on a 400 MHz solid-state NMR spectrometer (Bruker, DSX400 WB). ¹³C NMR CP/MAS spectra were measured at a spinning speed of 6.5 kHz and a scanning range from 180 to -10 ppm using a 25 kHz spectral width (5.0 μ s 90° pulses) with a contact time of 1 ms and a delay time of 2 s.

Morphological Characterization. Transmission electron microscopy (TEM) was used to evaluate the dispersion of silica within the PLA matrix. The observations were performed on ultrathin sections of microtomed composite films with a Hitachi H-7100 using an acceleration voltage of 75 kV.

Characterization and Thermal Analysis. The grafting degree of modified silica and thermal stability of the composites were determined using a Thermogravimetric Analyser (TGA; Perkin Elmer, Pyris 1) with a heating rate of 20°C/min from 50 to 800°C in a nitrogen environment. The grafting degree GX (GPS grafting) and PX (PEG grafting; %) were roughly estimated based on the literature²² given below. For GPS-silica case, GX is equal to $(W_x - W_s)/(W_g - W_s)$, where W_x , W_g , and W_s are the residual weight difference (wt %) of epoxy silane-modified silica, GPS, unmodified silica, respectively, at the temperature between 100 and 800°C. For mPEG750-silica case, PX is equal to $(W_{px} - W_{gs})/(W_p - W_{gs})$, where W_{px} , W_p , and W_{gs} are the residual weight difference (wt %) of PEG-modified silica, PEG, GPS-modified silica, respectively.

The glass transition temperature (T_g) was determined using a differential scanning calorimetry (TA DSC, Q10) at a heating rate of 20°C/min from -10 to 200°C. In addition, a dynamic mechanical analyzer (Perkin Elmer, Pyris Diamond) was used to confirm T_g (Peak value of $\tan \delta$ through the ratio of dynamic

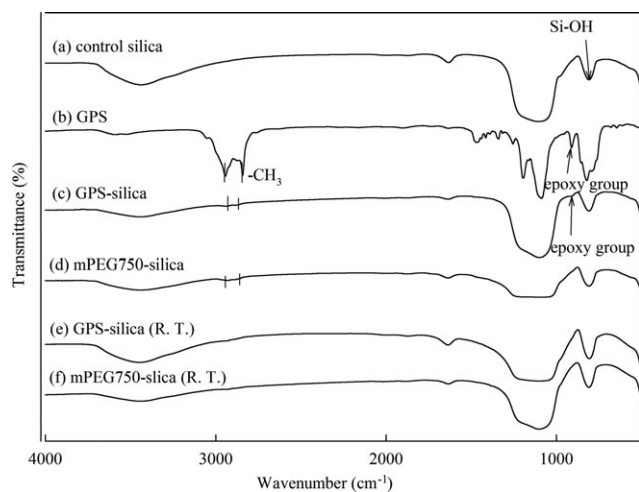


Figure 1. FTIR spectra of control silica, GPS-silica, and mPEG750-silica.

loss modulus to storage modulus) under a 3-point bending mode at a frequency of 1 Hz and at a heating rate of 2°C/min from 25 to 100°C.

Mechanical Properties. Tensile measurements were conducted based on ASTM-D368 at a crosshead speed of 5 mm/min using an Instron 4469. Tensile strength, elongation at break, and Young's modulus were recorded.

Optical Transmittance. The Optical property was evaluated using a UV-visible light spectrophotometer (HITACHI, U2010) with a scanning wavelength from 200 to 900 nm for 1 mm thick samples.

RESULTS AND DISCUSSION

Structure and Thermal Characterization of Modified Silica

To ensure a successful grafting reaction of silane (GPS) onto silica, FTIR was employed to determine the targeted functional groups. Major regions of the FTIR spectra of silica with or without mPEG modification are depicted in Figure 1 for comparison. The stretching of Si—OH bonds at 960 cm^{-1} was the characteristic band of control silica. After the epoxy silane grafting reaction, the characteristic absorption regions of GPS-silica on C—H groups (2947 cm^{-1} and 2895 cm^{-1}), and epoxy peak (910 cm^{-1}) are not clearly observed due to the resolution of curves as indicated in the literature.²³ Therefore, the grafting reaction of GPS-silica was also conducted at room temperature for comparison. Clearly, if one takes a close look on the curves, the cases of high grafting ratio of GPS in the regular grafting process did show broad bands of C—H bonding [Figure 1(c)], but no visible C—H peaks for the additional work on the grafting of GPS prepared at room temperature [Figure 1(e)] were observed. Basically, the results confirmed the effective grafting of epoxy silane. After GPS-silica reacted with mPEG further, the characteristic absorption of epoxy peak disappeared through the epoxy ring of GPS-silica and OH group of mPEG. Similarly, high grafting ratio of mPEG in the regular grafting process did show broad bands of C—H bonding [Figure 1(d)], but no visible C—H peaks for the additional work on the grafting of mPEG onto GPS-silica prepared at room temperature [Figure

1(f)] were observed. Thus, the effective grafting of mPEG onto silica was justified. However, the later evaluation on the weight loss of GPS-silica and mPEG-silica prepared at room temperature still showed some grafted/coated mixtures of surface modifiers on the silica surfaces resulting from the strong silanol reaction between silica and silane.

To get further, the detail of modified silica structure, ^{13}C CP/MAS NMR to probe the information of carbon environment was employed, as shown in Figure 2. There were no carbon traces for control silica particles. After epoxy silane treatment, six major resonance peaks from epoxy silane were observed at 10 ppm (α), 23 ppm (β), 72 ppm (γ), 74 ppm (δ), 53 ppm (ϵ , epoxy ring), and 44 ppm (ζ , epoxy ring).²⁴ Owing to the reaction of epoxy group and hydroxyl group on mPEG, additional characteristic peaks associated with methyl ether terminal group 59 ppm (κ) in accompany with a shift of peaks at 62 ppm (θ) and 64 ppm (η) were observed for mPEG-modified silica.²⁵ The characteristic epoxy ring bands disappeared, as observed in the literature.²¹ Besides, peaks around 70–75 ppm (γ , ι) represented the characteristic of carbon atoms in mPEG as well.²⁵ The current results suggested a successful grafting of mPEG onto silica through the help of epoxy silane via a ring-opening reaction.

TGA was employed to estimate roughly the grafting degree of mPEG onto silica. Figure 3 show the thermal scan of silica under different modification steps. For control silica, the grafting degree of organic moiety was virtually zero. With GPS modification, the grafting degree of GPS was calculated to be about 10.6 wt % based on the literature.²² For mPEG750-silica case, the grafting degree increased further to 19.8 wt %, indicating that mPEG was successfully grafted onto the silica surface in agreement with FTIR and NMR analyses. In addition, we attempted to employ the lower grafting temperature for the reaction between GPS and silica to check if any GPS could be grafted on the silica surface. Only 3.1 wt % of GPS was literally existed on silica surface as shown in Figure 3. The further reaction of GPS-silica and mPEG remained unchanged, so the grafted mPEG was quite limited as well. Thus, these additional experimental results reflected that our high temperature grafting process was quite effective and not a simple coating process, especially after a thorough wash.

Dispersion Assessment

TEM experiments were carried out to delineate the dispersion status of the control and organically modified silica in the PLA matrix. The agglomerated dark particles represent silica particles and the gray base represents the PLA matrix. Figure 4(a–c) show TEM morphology of PLA/silica nanocomposites for control silica at 1, 4, and 10 phr, respectively. Due to a low aggregation tendency of this novel commercial nanosilica, only a slight agglomeration of about a few hundred nm in size was observed in the PLA matrix. Figure 4(d–f) show TEM morphology of PLA/mPEG750-silica nanocomposites for mPEG750-silica at 1, 4, and 10 phr, respectively, at a magnification of 100 kx. It was noticed that the dispersion degree of modified silica cases appeared to be slightly improved, attributing to the certain grafting degree of mPEG onto silica surface. However, strictly speaking, the difference was kind of limited. Thus, the later

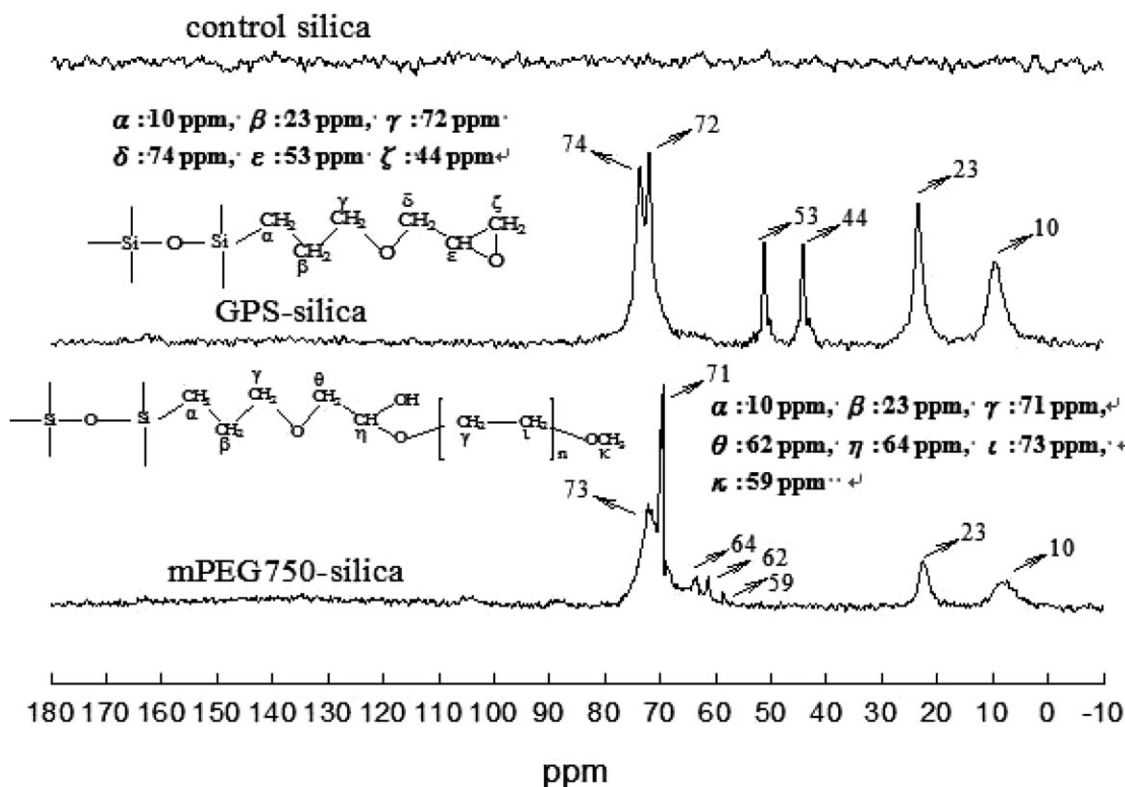


Figure 2. ^{13}C CP MAS NMR spectra of modified silica.

discussion on other properties signified the importance of the surface modification at a similar dispersion degree of silica within the PLA matrix.

Optical Properties

Figure 5 shows the optical transmittance of the PLA/silica nanocomposites to get some understanding on the optical transmittance effect through the incorporated inorganic fillers. As reported in the literature, three major factors governed the optical properties of polymer composites, inclusive of matrix properties, the interfacial refractive index difference between matrix and domains, and the size of dispersed domains.²⁶ The optical transmittance for pristine PLA was about 80% depending on the wavelength of visible light and was generally in a similar order as PLA/control silica cases at various silica contents in Figure 5(a). This indicated that the dispersion size of control silica within the PLA matrix was mainly in a nanoscale without interfering much on the scattering of visible light, which agreed with previous TEM observations. With the addition of surface-modified silica, the optical transmittance remained largely the same at various silica contents over the scanning wavelength of visible light as above cases within experimental errors, as seen in Figure 5(b). The results were in line with the morphology observation, leading to a similar dispersion scale for all surface-modified silica and control silica. Therefore, the further discussion on the properties of prepared nanocomposites was mainly attributed to the surface modifier effect in general.

Thermal Behaviors

It is worth checking how the thermal behaviors varied with the mPEG modification for silica-filled nanocomposites. Although silica was considered as an effective nucleating agent, the promotion of crystallization kinetics through the addition of silica moiety was still limited. No crystallization behaviors were observed for neat PLA and PLA nanocomposites at various silica contents with or without mPEG modification (omit here for brevity). The heating thermographs of PLA/silica nanocomposites are shown in Figure 6. The glass transition temperature

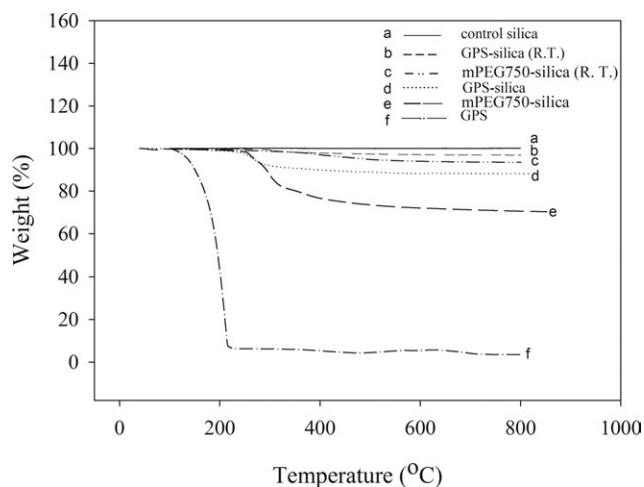


Figure 3. TGA of modified silica.

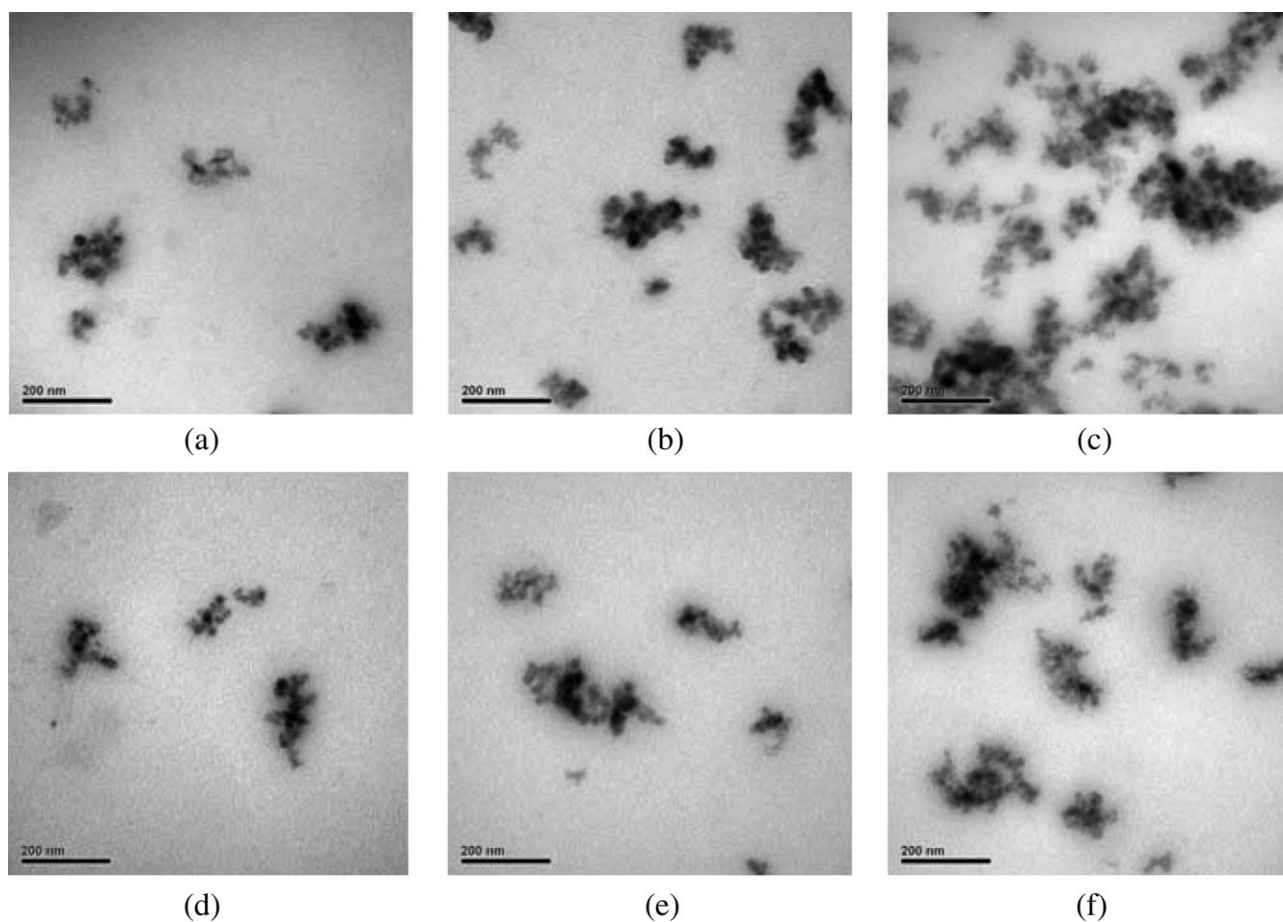


Figure 4. TEM micrographs of PLA/silica nanocomposites: (a–c) control silica and (d–f) mPEG750-silica (scale bar: 200 nm).

for neat PLA was at 58.5°C, which was about the same as those of PLA containing various dosages of silica. Not much difference in the glass transition temperatures was found for PLA/control silica systems. When the measurements were conducted at various dosages of mPEG750-silica as shown in Figure 6(b), the glass transition temperature of PLA/mPEG750-silica nanocomposites at 10 phr of modified silica was shifted to the lower temperature at 47.6°C, up to about 11°C decrement. Consequently, the mPEG plasticizer efficiently plasticized the PLA matrix due to the enhanced segmental mobility of PLA chains,²⁷ and the plasticizing degree of which was enhanced with higher plasticizer content.

Figure 7 shows the temperature dependency of $\tan \delta$ for PLA/silica nanocomposites at various silica contents with or without mPEG modification. The glass transition peaks reflected in the $\tan \delta$ values that were quite intensive for prepared systems. The $\tan \delta$ peak temperature for neat PLA was at 60.1°C. With the addition of control silica, the $\tan \delta$ peak varied less than 1°C within experimental error. Nevertheless, for PLA/mPEG750-silica systems, the $\tan \delta$ peak temperature at 10 phr of mPEG-modified silica was shifted to lower temperature at 53.8°C. This trend was in agreement with the DSC measurement to signify the plasticizing effect of grafted mPEG onto silica, although DMA gave slightly smaller difference in the glass transition temperatures after modification.

Thermal Stability

TGA was employed to evaluate the thermal stability of PLA/silica nanocomposites. Figure 8 shows the thermal scans of PLA nanocomposites at various silica dosages. The incorporated silica improved the thermal stability of PLA nanocomposites as heat and oxygen barrier normally found in the inorganic silica-filled nanocomposite systems. Taking the 5 wt % of weight loss as an index of thermal stability, as shown in Table I, the degradation temperature increased from 317.5°C for neat PLA to 355.4°C for the PLA/control silica nanocomposite in the 10 phr-loaded system and to 325.4°C for the PLA/mPEG750-silica nanocomposite in the 10 phr-loaded system, respectively. The effect of filled silica with or without modification on the thermal stability increased with increasing silica content, but the incorporated mPEG appeared to discount the thermal stability of PLA nanocomposites. Further, the other representative degradation temperatures are also shown in Table I for quick comparison. A similar conclusion was drawn for the both silica-reinforced cases.

Mechanical Properties

As pointed out earlier in the TEM morphology, PLA/control silica and PLA/mPEG750-silica nanocomposites all displayed a similar dispersion degree in the TEM images, especially for low silica dosages. It is interesting to see how the modified silica affects the mechanical properties of prepared nanocomposites.

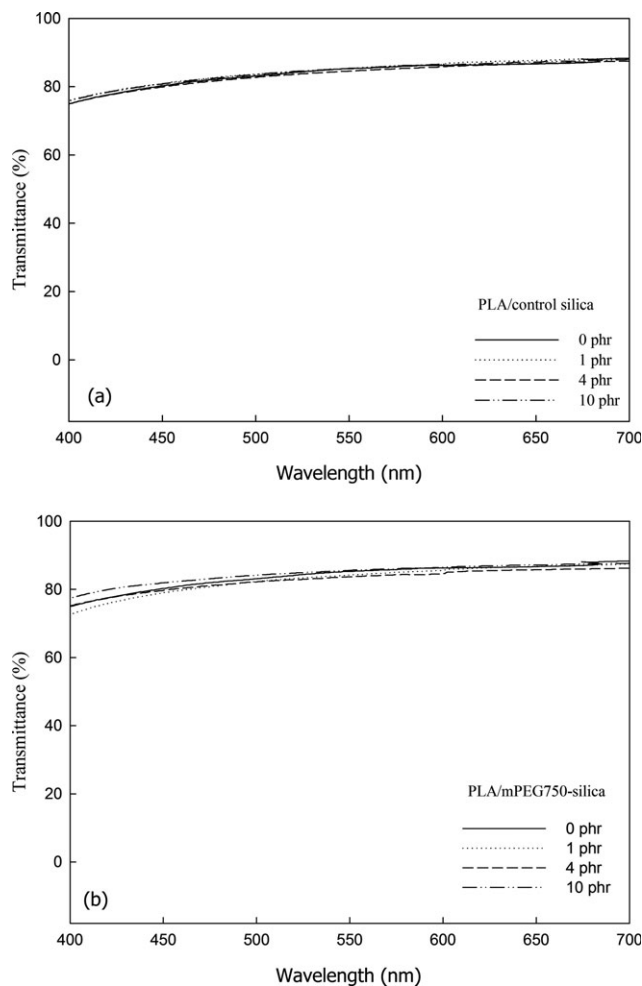


Figure 5. Transmittance of PLA/silica nanocomposites: (a) control silica and (b) mPEG750-silica.

The results of tensile properties are illustrated in Figure 9. Figure 9(a) depicts Young's modulus of nanocomposites. Young's modulus of PLA was about 2133 ± 53 MPa, and the value for the nanocomposite at 10 phr of control silica increased up to 2547 ± 54 MPa mainly due to the reinforcing effect from nanoparticles. For modified silica, Young's modulus decreased at various silica contents, attributing to the plasticizing effect from the grafted mPEG. This signifies the importance of surface modifier effect at similar silica dispersion in the prepared systems.

To further contrast the performance of the modified silica on the tensile properties of the nanocomposites, Figure 9(b) shows the tensile strength varied with silica dosages. Again, incorporated silica enhanced tensile strength for the control silica-filled nanocomposites. Tensile strength of neat PLA was about 53.9 ± 4.1 MPa, and the value for the nanocomposites increased up to 60.7 ± 3.0 MPa at 10 phr of control silica due to the reinforcing effect of inorganic nanoparticles, as discussed in the modulus section. However, tensile strength for nanocomposites containing modified silica was lower than that of neat PLA, a similar trend as seen in Young's modulus. This was attributed to the plasticizing effect of surface modifier, which implied the

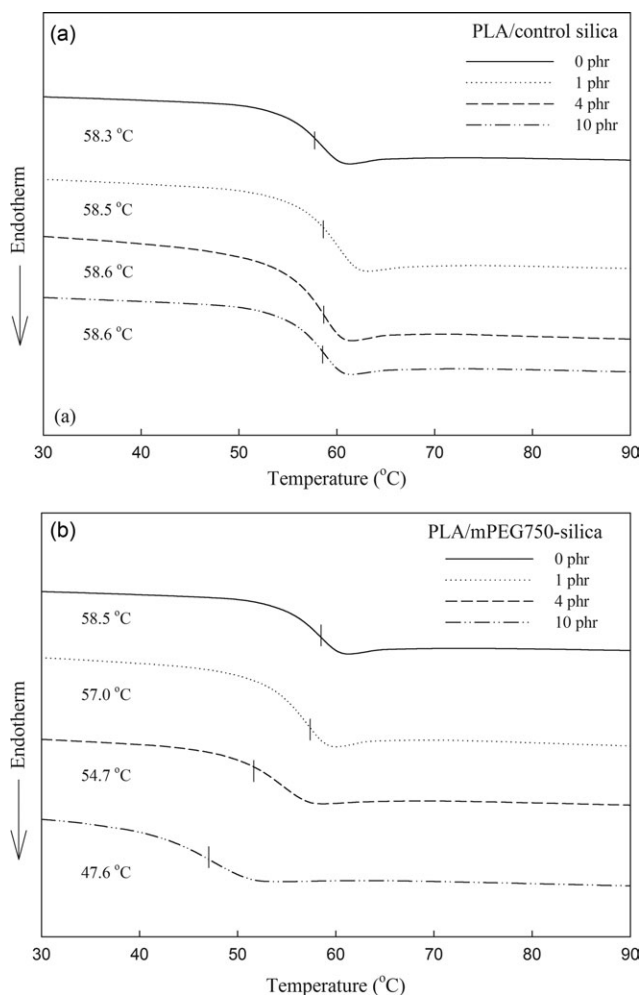


Figure 6. DSC thermographs of PLA/silica nanocomposites: (a) control silica and (b) mPEG750-silica.

significance of the surface modification. For small deformation as in the case of Young's modulus and large deformation as in tensile strength, the surface modification played an important

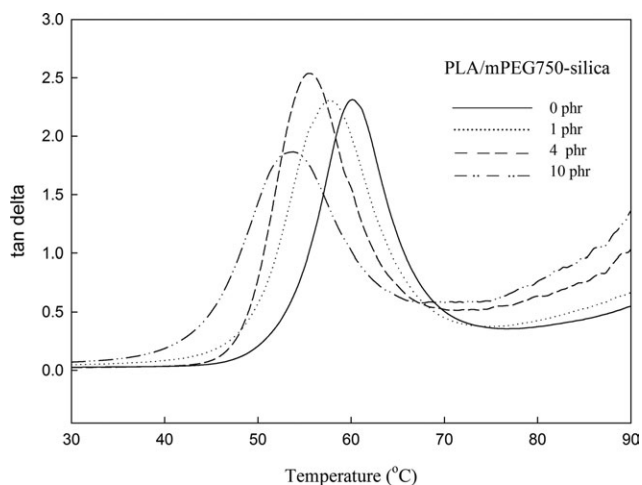


Figure 7. Tan δ of PLA/silica nanocomposites varied with temperature.

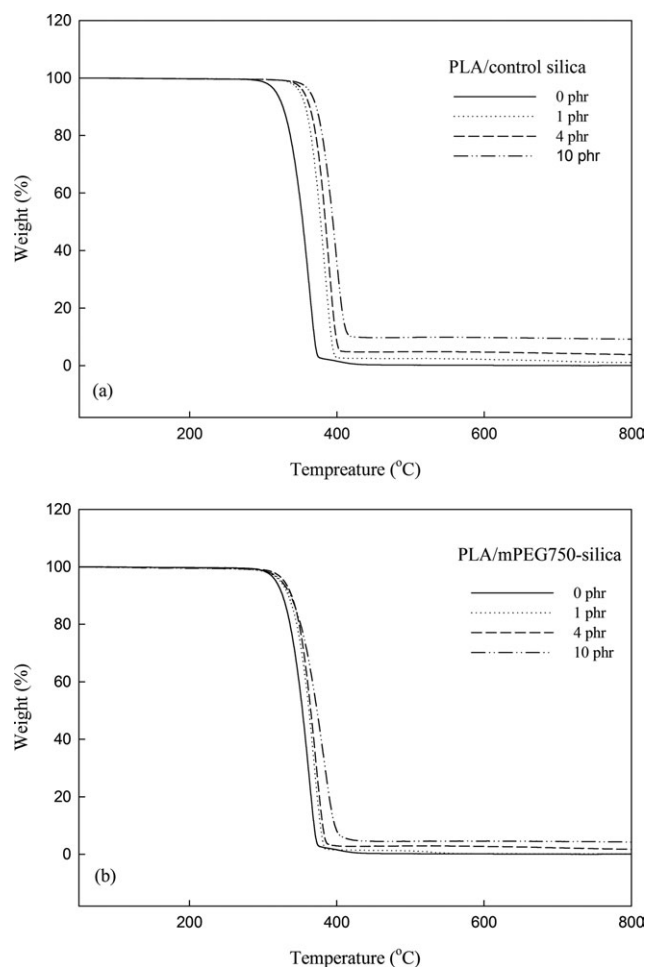


Figure 8. Thermogravimetric curves of PLA/silica nanocomposites.

role, even though there was a similar dispersion degree of incorporated silica.

To further contrast the plasticizing performance of the modified silica on the tensile properties of the nanocomposites, Figure

Table I. Thermal Degradation Temperatures of PLA with Different Silica Concentrations

Sample code	Weight loss temperature (°C) at the loss of	
	5 wt %	50 wt %
PLA	317.5	353.7
PLA/control silica (phr)		
1	349.7	378.0
4	349.9	384.2
10	355.4	394.3
PLA/mPEG750-silica (phr)		
1	323.3	362.3
4	328.6	365.0
10	325.4	373.3

Note: The denotation of parts per hundred resins and fillers (‘phr’) is based on the hundred parts of total amount of PLA.

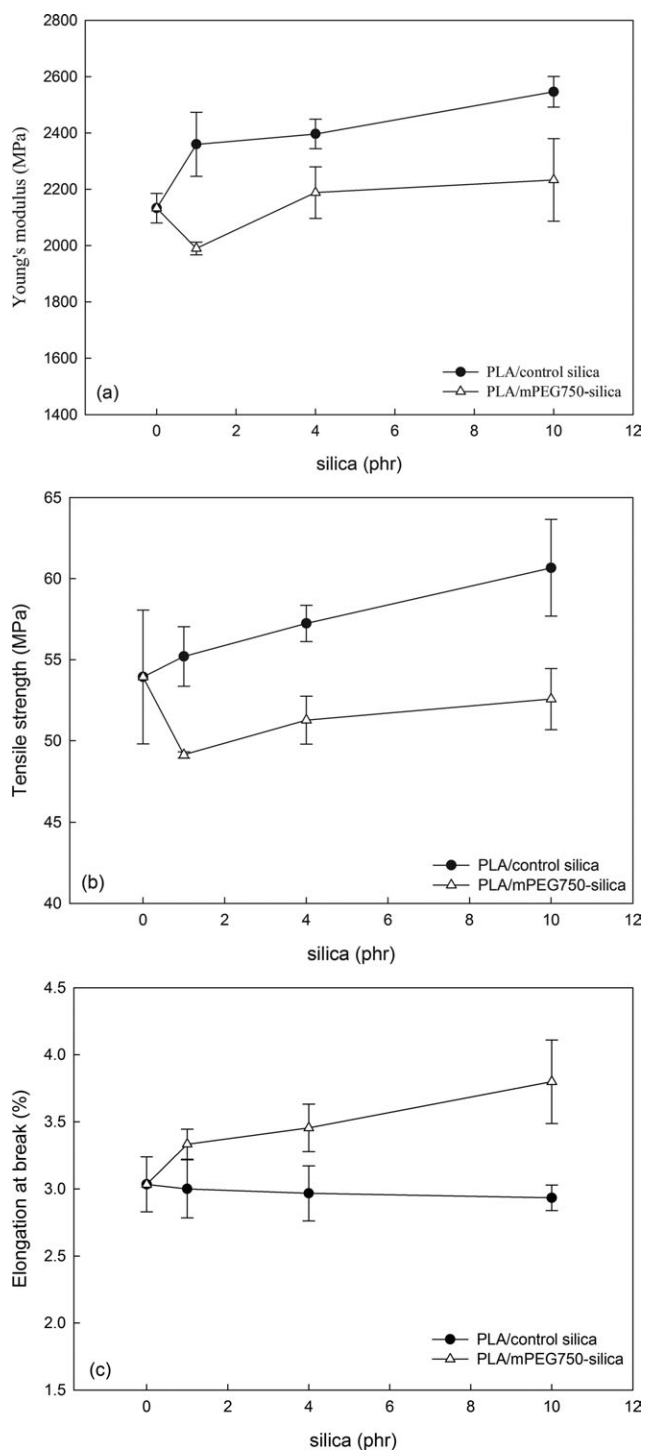


Figure 9. Mechanical properties of (a) Young's modulus, (b) tensile strength, and (c) elongation at break.

9(c) shows the elongation at break of the prepared nanocomposites varied with silica dosages. The elongation at break for control silica-filled cases was lower than that of modified silica-filled cases. Although the difference was not significant, it did signify the surface plasticizing effect of mPEG. This modified silica method in preparing plasticized silica-filled PLA nanocomposites was one of few studies^{13,16,19} to balance the

reinforcing effect from inorganic silica and plasticizing effect from the plasticizer, especially under a similar silica dispersion. In addition, the prevailing surface modification processes in the literature often led to high dispersion of silica, which made it hard to independently separate the surface modification effect and silica dispersion effect. Through the current approach, it is possible to solely consider the surface modification effect under the similar silica dispersion in general. Further study is necessary to increase the surface modifier content to exploit this novel approach.

CONCLUSIONS

The effect of surface modification of silica on the performance of PLA/silica nanocomposites was investigated. Two-step modification was carried out. At first, epoxy silane was grafted onto silica, and then the grafting reaction of mPEG onto epoxy grafted silica. The grafting percentage of mPEG onto silica was about 19.8 wt %. Transmission electron microscope revealed a similar dispersion degree for control silica and modified silica-filled PLA nanocomposites, especially at low silica dosages, which was in line with the optical transmittance measurement as well. Thus, a direct effect of the surface modifier on other properties could be elucidated under the similar silica dispersion after modification. Not much difference in the glass transition temperatures was found for PLA/control silica systems, yet the glass transition temperature of PLA/mPEG750-silica nanocomposite at 10 phr of modified silica was shifted to the lower temperature at 47.6°C. Consequently, the mPEG plasticizer efficiently plasticized the PLA matrix due to the enhanced segmental mobility of PLA chains, in agreement with the DSC measurement. Young's modulus of PLA was about 2133 ± 53 MPa, and the value for the nanocomposite increased up to 2547 ± 54 MPa at 10 phr of control silica mainly due to the reinforcing effect from nanoparticles. For modified silica, Young's modulus decreased at various silica contents. Tensile strength for nanocomposites containing modified silica was lower than that of neat PLA, a similar trend as seen in Young's modulus. This was attributed to the plasticizing effect of surface modifier, which implied the significance of the surface modification. The elongation at break for modified silica-filled cases was higher than that of control silica-filled cases. Although the difference was not significant, it did signify the surface plasticizing effect of mPEG. This study could pave the way for the future development of bio-based PLA/silica nanocomposites in the potential applications, such as foam, film, etc., in light of balancing the reinforcing and plasticizing effects under similar silica dispersion.

ACKNOWLEDGMENTS

Grants-in-aid from R.O.C. government under the contract number of NSC 99-2221-E-197-006- and NSC 100-2120-S-197-001-NM are greatly acknowledged. The authors are also grateful to Mr. Mu-Yu Chou for the assistance in the preparation of revised manuscript.

REFERENCES

1. Philipp, G.; Schmidt, H. *J. Non-Cryst. Solids* **1984**, *63*, 283.
2. Wilkes, G. L.; Orler, B.; Huang, H. *Polym. Prep.* **1985**, *26*, 300.
3. Kweon, D.-K.; Cha, D.-S.; Park, H.-J.; Lim, S.-T. *J. Appl. Polym. Sci.* **2000**, *78*, 986.
4. Ray, S. S.; Okamoto, M. *Macromol. Rapid. Commun.* **2003**, *24*, 815.
5. Gu, S.-Y.; Ren, J.; Dong, B. *J. Polym. Sci. Part B: Polym. Phys.* **2007**, *45*, 3189.
6. Petersson, L.; Oksman, K.; Mathew, A. P. *J. Appl. Polym. Sci.* **2006**, *102*, 1852.
7. Li, T.; Turng, L.-S. *Polym. Eng. Sci.* **2006**, *46*, 1419.
8. Nieddu, E.; Mazzucco, L.; Gentile, P.; Benko, T.; Balbo, V.; Mandrile, R.; Ciardelli, G. *React. Funct. Polym.* **2009**, *69*, 371.
9. Arroyo, O. H.; Huneault, M. A.; Favis, B. D.; Bureau, M. N. *Polym. Compos.* **2010**, *31*, 114.
10. Zhou, Q.; Xanthos, M. *Polym. Eng. Sci.* **2010**, *50*, 320.
11. Picard, E.; Espuche, E.; Fulchiron, R. *Appl. Clay Sci.* **2011**, *53*, 58.
12. Wang, B.; Wan, T.; Zeng, W. *J. Appl. Polym. Sci.* **2011**, *121*, 1032.
13. Yan, S.; Yin, J.; Yang, Y.; Dai, Z.; Ma, J.; Chen, X. *Polymer* **2007**, *48*, 1688.
14. Wang, H.; Fang, M.; Shi, T.; Zhai, L.; Tang, C. *J. Appl. Polym. Sci.* **2006**, *102*, 679.
15. Zhang, J.; Lou, J.; Ilias, S.; Krishnamachari, P.; Yan, J. *Polymer* **2008**, *49*, 2381.
16. Yan, S.; Yin, J.; Yang, J.; Chen, X. *Mater. Lett.* **2007**, *61*, 2683.
17. Huang, J.-W.; Hung, Y. C.; Wen, Y.-L.; Kang, C.-C.; Yeh, M.-Y. *J. Appl. Polym. Sci.* **2009**, *112*, 1688.
18. Huang, J.-W.; Hung, Y. C.; Wen, Y.-L.; Kang, C.-C.; Yeh, M.-Y. *J. Appl. Polym. Sci.* **2009**, *112*, 3149.
19. Zhu, A.; Diao, H.; Rong, Q.; Cai, A. *J. Appl. Polym. Sci.* **2010**, *116*, 2866.
20. Fukushima, K.; Tabuani, D.; Abbate, C.; Arena, M.; Rizzarelli, P. *Eur. Polym. J.* **2011**, *47*, 139.
21. Huang, W.; Zhou, Y.; Yan, D. *J. Polym. Sci. Part A: Polym. Chem.* **2005**, *43*, 2038.
22. Guo, Y.; Wang, M.; Zang, H.; Liu, G.; Zhang, L.; Qu, X. *J. Appl. Polym. Sci.* **2008**, *107*, 2671.
23. Isin, D.; Kayaman-Apohan, N.; Gungor, A. *Prog. Org. Coat.* **2009**, *65*, 477.
24. Davis, S. R.; Brough, A. R.; Atkinson, A. *J. Non-Cryst. Solids* **2003**, *315*, 197.
25. Innocenzi, P.; Brusatin, G. *Chem. Mater.* **2000**, *12*, 3726.
26. Wang, S.; Zhang, Y.; Ren, W.; Zhang, Y.; Lin, H. *Polym. Test.* **2005**, *24*, 766.
27. Kulinski, Z.; Piorkowska, E.; Gadzinowska, K.; Stasiak, M. *Biomacromolecules* **2006**, *7*, 2128.